New Journal of Physics
The open-access journal for physics

Optimization of laser field-free orientation of a state-selected NO molecular sample

Arnaud Rouzée[1,4], Arjan Gijsbertsen[1], Omair Ghafur[1], Ofer M Shir[2], Thomas Bäck[2], Steven Stolte[3] and Marc J J Vrakking[1]

[1] FOM Institute for Atomic and Molecular Physics (AMOLF), Science Park 113, 1098 XG Amsterdam, The Netherlands
[2] Leiden Institute of Advanced Computer Science (LIACS), Niels Bohrweg 1, 2333 CA Leiden, The Netherlands
[3] Vrije Universiteit Amsterdam De Boelelaan 1083, 1081 HV Amsterdam, The Netherlands, Laboratoire Francis Perrin, Bâtiment 522, DRECAM/SPAM/CEA Saclay, 91191 Gif sur Yvette, France and Institute of Atomic and Molecular Physics, Jilin University, Changchun 130012, People's Republic of China
E-mail: a.rouzee@amolf.nl

New Journal of Physics **11** (2009) 105040 (19pp)
Received 19 May 2009
Published 30 October 2009
Online at http://www.njp.org/
doi:10.1088/1367-2630/11/10/105040

Abstract. We present a theoretical investigation of the impulsive orientation that can be induced by exposing a sample of state-selected NO molecules to the combination of a dc field and a short laser pulse. A strong degree of laser-field-free alignment and orientation is already achievable at moderate intensities and can be further improved by tailoring the temporal profile of the laser pulse. The alignment and orientation are only limited by the maximum value of the applied dc field and the pulse energy in the femtosecond laser pulse. Using an evolutionary algorithm coupled to a non-perturbative calculation of the time-dependent Schrödinger equation, the solutions that are obtained suggest that $\langle \cos\theta \rangle = 0.964$ is experimentally achievable.

[4] Author to whom any correspondence should be addressed.

Contents

1. Introduction

In the past few decades the chemical and physics community has shown considerable interest in the alignment and orientation of molecular samples. Processes such as bi-molecular collisions (chemical reactions) and photon–molecule collisions are highly sensitive to the relative arrangement of the collision partners. Molecular alignment and orientation provide a means towards detailed investigations of this stereo-specificity, as well as a route towards controlling the outcome of the collision, which is a long-standing goal in the molecular sciences.

A molecular sample is considered to be oriented when its angular distribution is asymmetric upon reflection ($\langle\cos\theta\rangle \neq 0$, with θ the angle between the molecular axis and the fixed in space laboratory axis), while it is considered to be aligned if this distribution is symmetric but not isotropic ($\langle\cos^2\theta\rangle \neq 1/3$). Orientation and alignment often go hand-in-hand, although this is not necessarily the case. Over the years, techniques to control alignment and orientation have progressed from orientation in electrostatic fields [1]–[3] to laser control over alignment [4]–[7] and orientation [8]–[11]. Using electrostatic fields, two common experimental methods exist to orient molecules, namely the hexapole state selection [1, 12, 13] and brute-force orientation techniques [14, 15]. In the former, a moderately strong electrostatic field (typically 0.1–20 kV cm^{-1}, depending on the magnitude of the permanent dipole moment and the rotational constant) is applied to dipolar molecules in a specific ro-vibrational state, which is selected by passage of the molecules through a hexapole structure. Far stronger electric fields are necessary in the brute-force technique that exploits the second- and higher-order Stark effects (see [16] for a comparison between hexapole state selection and brute force orientation).

Research on molecular alignment due to intense laser fields was triggered in 1992 by Normand *et al* [17], who claimed that an intense laser field forces molecules to align along its polarization vector. They performed experiments where CO molecules were dissociatively ionized using an intense femtosecond laser and observed that the fragment ions were preferentially ejected along the laser polarization axis. Two possible explanations were offered for this observation, namely geometric and dynamic alignment. Geometric alignment corresponds to an alignment of the fragment ion distribution due to the larger ionization probability of molecules that are aligned along the laser polarization axis. Dynamic alignment corresponds to alignment arising from the dipole that is induced in a molecule by a laser and the torque on the molecule that arises as a result of the interaction of this dipole with the laser electric field. In 1995, Friedrich and Herschbach published a rigorous theoretical treatment [4] of dynamic molecular alignment in an intense laser field, which motivated many subsequent

theoretical and experimental investigations on laser-induced alignment of molecules [18]. An early demonstration of laser-induced molecular alignment was performed by Stapelfeldt and co-workers [19, 20] in an adiabatic regime, where the laser pulse is long compared to the rotational period of the molecule. Then molecules are aligned while the laser pulse is present, and the molecule returns to its initial free rotor state after the laser pulse, at which the alignment again vanishes. Unlike techniques that are based on electrostatic fields, the use of laser excitation also allows one to accomplish alignment and orientation under field-free conditions. This is advantageous, since the presence of strong electric fields may influence the chemical or physical processes that one wishes to study using the aligned/oriented molecules. We previously demonstrated that molecules can be non-adiabatically (impulsively) aligned employing laser pulses that are short compared to their rotational period [6]. Periodic alignment revivals then occur that can be understood in terms of the formation of a coherent superposition of rotational states that is aligned upon turn-off of the laser and that subsequently de-phases and revives periodically [21]. The degree of alignment that is achievable using a short laser excitation pulse has been shown to be limited but can be increased by making use of a laser pulse sequence with suitable chosen delays between the pulse [22, 23] or by tailoring the temporal profile of the pulse by a pulse shaping device such as a spatial light modulator (SLM) [24, 25]. Currently, many applications are being developed where field-free laser-induced alignment is being put to use, including experiments where high harmonic generation [26] or electron tunneling and diffraction [27] is used to determine the nuclear [28, 29] and electronic [30] structure of molecules.

With the theoretical and experimental work on laser-induced molecular alignment now becoming increasingly mature, including also the (three-dimensional) alignment of asymmetric top molecules like 3,4-dibromothiophene and 3,5-difluoroiodobenzene [31, 32], SO_2 [33] or ethylene [34, 35], researchers are presently beginning to turn their attention towards laser-based orientation of molecules. In an early proposal towards this goal, we have considered a scheme to orient either (hexapole) state-selected molecules or a rotationally cold sample of molecules by two-color phase-locked laser excitation [8]. A superposition of both negative and positive parity levels can then be formed in the ground electronic state, which leads to a macroscopic orientation both during and after the laser pulse. In the case of hexapole state-selected NO, where the negative and positive parity components are the two levels of the ground state Λ-doublet, the degree of orientation alternates and changes sign on a nanosecond timescale. When preparing a mixed parity coherent superposition of ground rotational states starting from a rotationally cold sample, the evolution of the orientation is significantly more rapid and is determined by the rotational period of the molecule. Other approaches to achieve molecular orientation using a two-color phase locked laser pulse, which have been investigated theoretically, include work by Dion [36] and Kanai *et al* [37], who proposed use of vibrational resonance and non-resonant excitation, respectively.

Half-cycle THz pulses, used either by themselves [38, 39] or in combination with a second (non-resonant) laser pulse [40, 41] have also been considered for achieving impulsive orientation. The half-cycle pulse is short compared to the rotational period of the molecule and imparts a kick to the molecule, creating a mixed parity rotational wave packet. It was demonstrated numerically that orientation revivals may occur after the half-cycle pulse. Although the required field strengths for achieving impulsive THz orientation have thus far not been available, the technique is nevertheless promising in light of significant recent improvements in THz generation technology [42] at accelerator facilities. Specifically, the

integration of intense THz pulses at XUV/x-ray free electron laser facilities that are currently under development offers exciting prospects for future research.

Friedrich and Herschbach realized that a combination of an electrostatic and a non-resonant laser field could enhance the degree of (brute force) orientation [43]–[45]. The initial demonstration of this method was provided by Buck and co-workers [9], followed by Sakai *et al* [10]. Latter, Tanji *et al* used an elliptically polarized laser pulse combined with a dc field to achieve three-dimensional orientation [46]. Also, all these experiments were done in an adiabatic regime where the orientation is lost when the laser turns off. More recently, these same authors have exploited the rapid turn-off of a long laser pulse to induce the formation of a rotational wave packet that displays revivals similar to those that are created by a short pulse [47]. The measured degree of orientation in this experiment was modest due to the incoherent de-phasing induced by the presence of many different rotational states in the initial sample. Two recent experiments have addressed this issue and have thereby been able to achieve considerably higher degrees of orientation. In the experiment of Holmegaard *et al*, a strong static inhomogeneous electric field was used to spatially disperse a sample of polar molecules, thereby allowing the selection of a subset of molecules that could be adiabatically aligned and oriented [48]. In our own recent work [49] we have applied hexapole state-selection of a single rotational state of NO with the application of a moderate dc electric field and a shaped femtosecond laser pulse, in order to achieve an unprecedented degree ($\langle\cos\theta\rangle = -0.74$) of laser field-free orientation.

The purpose of the present paper is to provide the theoretical basis for the experimental results that were presented in [49] and to explore to what extent the degree of orientation can be further increased. We present calculations where the degree of orientation is numerically optimized using an evolutionary strategy, leading to the conclusion that under realistic, experimentally achievable conditions, $\langle\cos\theta\rangle = 0.964$ should be achievable.

2. Hexapole state-selection, dc and laser field orientation

Before proceeding to discuss our computational approach to characterize impulsive molecular orientation and alignment, it is useful to briefly discuss the rotational structure of the NO molecule. NO has an odd number of electrons and a nonzero electronic orbital angular momentum. Consequently, it has a degenerate $^2\Pi$ open shell in its ground electronic state that results in half-integer J values, where J is the total angular momentum of the molecule. The ground state is split into $^2\Pi_{1/2}$ and $^2\Pi_{3/2}$ components. In the rigid rotor approximation the molecule is described by the Hamiltonian that includes the spin–orbit coupling [50]

$$\mathcal{H}_0 = \mathcal{H}_{\rm rot} + \mathcal{H}_{\rm SO} = B(\boldsymbol{J} - \boldsymbol{S} - \boldsymbol{L})^2 + A(\boldsymbol{L}\cdot\boldsymbol{S}), \tag{1}$$

with $\boldsymbol{J}$, $\boldsymbol{S}$ and $\boldsymbol{L}$ that represent, respectively, the quantum mechanical operators of the total angular momentum, the electronic spin and the electronic orbital angular momentum. The first term in this expression corresponds to the rotational motion and the second to the spin–orbit interaction. $B = 1.6961\,\mathrm{cm}^{-1}$ and $A = 123.13\,\mathrm{cm}^{-1}$ are, respectively, the rotational and the spin–orbit constant of the molecule. Note that in this expression the Λ type doubling is neglected. The eigenfunctions of the Hamiltonian (1) in the—for our purpose appropriate—approximation of Hund's case (a) coupling are expressed as:

$$|J, \bar{\Omega}, M, \epsilon\rangle = |J, \bar{\Omega}, M\rangle + \epsilon|J, -\bar{\Omega}, M\rangle, \tag{2}$$

where $|J, \pm\bar{\Omega}, M\rangle$ represents the wave function of a symmetric top molecule. J is the rotational angular momentum quantum number, $\bar{\Omega} \equiv |\Omega|$ is (the absolute value of) the projection of the total angular momentum $\boldsymbol{J}$ on a molecular frame axis, M is the projection of $\boldsymbol{J}$ on a space fixed axis and ϵ is a symmetry index ($\epsilon = -1, 1$). The wave function is given by

$$|J, \bar{\Omega}, M\rangle = \sqrt{\frac{2J+1}{4\pi}} D^J_{M,\bar{\Omega}}(\phi, \theta, 0). \tag{3}$$

with $D^J_{M,\bar{\Omega}}(\phi, \theta, 0)$ the usual rotation matrix. Since a diatomic molecule has only two rotational degrees of freedom, the last Euler angle χ is redundant and set to 0. The symmetry index ϵ relates to the total parity p of the rotational state as

$$p = (-1)^{J-\epsilon/2}. \tag{4}$$

The rotational energy levels that result from (1) and include the Λ-doublet splitting $W_\Lambda(J)$ between the states $|J, \bar{\Omega}, M, \epsilon = \pm 1\rangle$ are written as

$$E_{\text{rot}} = B\left[\left(J-\frac{1}{2}\right)\left(J+\frac{3}{2}\right) \pm \frac{1}{2}\sqrt{4\left(J+\frac{1}{2}\right)^2 + Y(Y-4) \mp (Y-2)}\right] - \frac{1}{2B}\epsilon W_\Lambda(J) \tag{5}$$

with $Y = \frac{A}{B}$. The $\pm$ in equation (5) distinguishes between the upper F_2 (dominated by $\bar{\Omega} = \frac{3}{2}$ if $A > 0$) and the lower F_1 (dominated by $\bar{\Omega} = \frac{1}{2}$ if $A > 0$) spin–orbit state. For NO, the two spin–orbit states—indicated by $^2\Pi_{\frac{1}{2}}$ and $^2\Pi_{\frac{3}{2}}$—differ about 121 cm^{-1} in energy, the latter having the highest energy. For the $^2\Pi_{\frac{1}{2}}$ states that are well approximated by Hund's case (a) coupling, the Λ-type splitting varies linearly with J. It can be approximated as

$$W_\Lambda = W_g\left(J+\frac{1}{2}\right). \tag{6}$$

Burrus and Gordy [51] obtained for the energy splitting of the $J = 1/2$ Λ-doublet $W_g = 0.0118\,\text{cm}^{-1}$.

As mentioned in the introduction, the hexapole method provides a convenient way to obtain a state-selected molecular sample. The technique of focusing polar molecules in a static electric field was developed in the 1950s and has subsequently been applied to many polar molecules [1, 12, 13]. Hexapole state-selection is based on the linear Stark shift that the energy levels of an atom or a dipolar molecule experience in an electrostatic field. The first-order Stark energy $W^{(1)}$ resulting from the interaction with the electrostatic field E_0 can be expressed as

$$W^{(1)} = -\mu_0 E_0 \langle\cos\theta_1\rangle, \tag{7}$$

where μ_0 is the permanent dipole moment and θ_1 is the angle between μ_0 and the electrostatic field E_0. In the case of NO, in a strong electrostatic field, the expectation value $\langle\cos\theta_1\rangle$ is well approximated by

$$\langle\cos\theta_1\rangle = \epsilon\frac{\overline{M\Omega}}{J(J+1)}. \tag{8}$$

These equations show immediately that molecules in different rotational states experience a different linear Stark shifts. In particular, molecules where $\epsilon = +1$ minimize their potential energy by moving towards higher field strengths (high-field seeking), while molecules in an $\epsilon = -1$ state are low-field seeking. Molecules in a low-field seeking state are pushed toward the center of the hexapole while molecules in a high-field seeking state are pushed away

from the symmetry axis of the hexapole. The hexapole acts therefore as a positive lens with a focal length that depends on the $|J, \Omega, M, \epsilon = -1\rangle$ rotational state of the molecules. After the supersonic expansion into a vacuum, the molecules primarily reside evenly in the two Λ-doublet components of the $(J = 1/2)$ rotational ground state. The hexapole focuses a beam of molecules in the low-field seeking state $|J = 1/2, \bar{\Omega} = 1/2, M = 1/2, \epsilon = -1\rangle$ into the interaction region (defined as the point where the NO beam intersects the laser beam).

After the hexapole, the molecules are state-selected but do not yet have a preferential orientation. In the experimental arrangement that we use (see figure 1 of [49]) the molecules enter a region where a moderately strong dc field is applied. In this dc field, the molecules again experience a Stark shift (see equation (6)), and consequently become oriented with respect to the dc electric field axis. Next, the molecules are exposed to a short laser pulse that is polarized along the dc electric field axis, leading to a significant enhancement of the orientation. If the laser pulse is shorter than the rotational period of the molecule, both revivals of the orientation and alignment are expected after the laser field has ended. The degree of orientation is quantified by $\langle \cos\theta \rangle$ (with θ the angle between the molecular and a space-fixed axis), while the degree of alignment is defined by $\langle \cos^2\theta \rangle$. Note that for an un-oriented sample $\langle \cos\theta \rangle = 0$, while for an un-aligned sample $\langle \cos^2\theta \rangle = 1/3$.

To quantify the degree of alignment and orientation, we consider that the molecules are subjected to both an electrostatic field E_O and a linearly polarized shaped laser field that is defined in the spectral domain as

$$E_A(t) = \frac{1}{2\pi} \int_{-\infty}^{+\infty} A(\omega) e^{i(\omega t + \phi(\omega))} d\omega, \tag{9}$$

where $\phi(\omega)$ and $A(\omega)$ denote the spectral phase and amplitude. Only phase shaping is applied in this work: $A(\omega)$ is kept constant and is taken to be a Gaussian centered at 800 nm with a width chosen such that the full-width at half-maximum (FWHM) of the corresponding Fourier transform limited (FTL, $\phi(\omega) = 0$) pulse is 100 fs. To reflect the pulse shaping process that is implemented experimentally by a SLM, the phase is specified by 128 parameters ϕ_n (pixels) taken as a top hat shape are equally distributed across the spectrum [24], i.e.

$$\phi(\omega) = \sum_{n=-63}^{64} \mathrm{squ}\left(\frac{\omega - \omega_n}{\Delta\omega}\right) \phi_n, \tag{10}$$

with the squ function reflecting the pixel shape:

$$\mathrm{squ}(x) = \begin{cases} 1, & \text{if } |x| \leqslant 1/2, \\ 0, & \text{if } |x| > 1/2. \end{cases} \tag{11}$$

Here, ω_n and ϕ_n correspond to the central (angular) frequency and the phase of the nth pixel, respectively. $\Delta\omega$ is the spectral sampling interval, i.e. the frequency difference between two adjacent pixels. In the calculations to be presented here $\Delta\omega = 0.8 \times 10^{12}\,\mathrm{rad\,s^{-1}}$.

As long as ω is far detuned from any vibronic transition frequencies, the effective potential induced by the dc and laser fields is well approximated by

$$V_{\mathrm{eff}} = V_O + V_A \tag{12}$$

where, similar to equation (7) V_O describes the interaction potential of the permanent dipole with the dc electric field

$$V_O = -\vec{\mu}_o \cdot \vec{E}_O \tag{13}$$

and V_A is the potential induced by the interaction of the laser with the anisotropic polarizability of the molecule [4, 21, 43]

$$V_A = -\tfrac{1}{2}(\vec{\vec{\alpha}} \cdot \vec{E}_A(t)) \cdot \vec{E}_A(t) = -\tfrac{1}{4}\Delta\alpha \mathcal{E}_A^2(t)\cos^2\theta, \tag{14}$$

with $\Delta\alpha = \alpha_\parallel - \alpha_\perp = 0.82\,\text{Å}^3$ the difference between the static polarizability parallel and perpendicular to the molecular axis and $\mathcal{E}_A(t)$ the temporal profile of the laser field. In expression (14), coupling terms that are independent of θ have been omitted since they do not affect the rotational dynamics. In dimensionless parameters, the effective potential of equation (12) can be written as

$$V_{\text{eff}} = -\omega_{E_O}\cos\theta - \Delta\omega_I\cos^2\theta, \tag{15}$$

with

$$\omega_{E_O} = \frac{\mu_o E_O}{B}; \quad \omega_{\parallel,\perp} = \frac{\alpha_{\parallel,\perp} I}{2B}; \quad \Delta\omega_I = \omega_\parallel - \omega_\perp = \frac{\Delta\alpha I}{2B}. \tag{16}$$

In these expressions, I is the time-dependent laser intensity. The selection rules for the excitation with a non-resonant laser pulse are $\Delta J = 0, \pm 1, \pm 2$, while the two quantum numbers $\bar{\Omega}$ and M are conserved during the process. Since Raman transitions require the conservation of overall parity, $\Delta J = 1$ transitions require that $\epsilon = -\epsilon'$, while $\Delta J = 2$ transitions can only occur if $\epsilon = \epsilon'$. The final Hamiltonian is therefore described by (note $M = M' = 1/2$ and $\bar{\Omega} = \bar{\Omega}' = 1/2$)

$$\begin{aligned} H_{J,J',\epsilon,\epsilon'} = \langle J',\ \bar{\Omega} = 1/2,\ M = 1/2,\ \epsilon' | H_{\text{rot}} - \omega_{E_O}\cos\theta \\ -\Delta\omega_I\cos^2\theta | J,\ \bar{\Omega} = 1/2,\ M = 1/2, \epsilon\rangle. \end{aligned} \tag{17}$$

The dynamics induced by the dc field alone is obtained by diagonalization of this expression without laser field. Considering only the linear Stark shift, the dc field mainly mixes the state that is selected by the hexapole into a combination of the $|J = 1/2, \bar{\Omega} = 1/2, M = 1/2, \epsilon = -1\rangle$ and $|J = 1/2, \bar{\Omega} = 1/2, M = 1/2, \epsilon = 1\rangle$ components of the Λ-doublet. The oriented wave function can thus be expressed as

$$|1/2, 1/2, 1/2, E_O\rangle = \alpha(E_O)|1/2, 1/2, 1/2, \epsilon = -1\rangle \pm \beta(E_O)|1/2, 1/2, 1/2, \epsilon = 1\rangle. \tag{18}$$

with $\alpha(E_O)^2 + \beta(E_O)^2 = 1$ [52]. For $E_O = 13\,\text{kV cm}^{-1}$ ($\omega_{E_O} = 0.021$), the mixing coefficients are $\alpha = 0.85$ and $\beta = 0.52$ and the degree of orientation is $\langle\cos\theta\rangle = 0.30$. A perfect mixing of the two parity component by the dc field ($\beta(E_O) = \alpha(E_O) = 0.5$) leads to the maximum orientation of ground state NO molecules $\langle\cos\theta\rangle = 1/3$. This is the value where the orientation saturates, at field strength $\gg 100\,\text{kV cm}^{-1}$ brute force orientation takes over.

The rotational dynamics of the molecule during and following the excitation with the pulse is evaluated by solving numerically the time-dependent Schrödinger equation during the laser pulse. The interaction leads to a rotational wave packet that evolves under field-free conditions after the laser pulse has ended at time t_f. We can expand the solution in a series of field free rotor wave functions

$$|\Psi(t)\rangle = \sum_{J,\epsilon} C_{J,\epsilon} e^{iE_{\text{rot}}(t-t_f)/\hbar} |J, \bar{\Omega} = 1/2, M = 1/2, \epsilon\rangle, \tag{19}$$

$$C_{J,\epsilon} = |C_{J,\epsilon}| e^{i\zeta_{J,\epsilon}}. \tag{20}$$

with E_{rot}, the energy of the molecule including the Stark shift induced by the dc field and neglecting the mixing between $\Delta J = \pm 1$ states that remains low for the dc field strength used

in the simulation. $\zeta_{J,\epsilon}$ represents the phase of each J,ϵ-component of the wave packet induced by the laser pulse (at t_f).

From expression (20) and appendix (A), one can evaluate the expectation values $\langle\cos^2\theta\rangle_t$ and $\langle\cos\theta\rangle_t$. We finally obtain

$$\langle\cos^2\theta\rangle_t = \sum_{J,\epsilon}|C_{J,\epsilon}|^2\alpha_{J,\epsilon} + 2\sum_{J,\epsilon}|C^*_{J+1,-\epsilon}C_{J,\epsilon}|\gamma_{J+1,\epsilon}\cos(\omega_{J+1,J}t+\zeta_{J+1,J}) + 2\sum_{J,\epsilon}|C^*_{J+2,\epsilon}C_{J,\epsilon}|\beta_{J+2,\epsilon}\cos(\omega_{J+2,J}t+\zeta_{J+2,J}) \quad (21)$$

and

$$\langle\cos\theta\rangle_t = \sum_{J,\epsilon}C^*_{J,-\epsilon}C_{J,\epsilon}\alpha'_{J,\epsilon} + 2\sum_{J,\epsilon}|C^*_{J+1,\epsilon}C_{J,\epsilon}|\gamma'_{J+1,\epsilon}\cos(\omega_{J+1,J}t+\zeta'_{J+1,J}). \quad (22)$$

In expression (21), $\alpha_{J,\epsilon}$, $\gamma_{J+1,\epsilon}$ and $\beta_{J+2,\epsilon}$ are matrix elements of $\cos^2\theta$ that couple states of same parity with $\Delta J=0$, $\Delta J=1$ and $\Delta J=2$, respectively, whereas in expression (22), $\alpha'_{J,\epsilon}$ and $\gamma'_{J+1,\epsilon}$ are the coupling terms between states with $\Delta J=0$ and 1, respectively, and with opposite parity. An analytical expression of those coefficients for all value of M and $\bar{\Omega}$ is derived in the appendix. $\omega_{J',J}$ are Raman frequencies that can be easily calculated using the expressions for $E_{\rm rot}$ given in (5), and $\zeta_{J+1,J}$ and $\zeta_{J+2,J}$ are defined using equation (20)

$$\zeta_{J+1,J} = \zeta_{J,\epsilon} - \zeta_{J+1,-\epsilon}, \quad (23)$$

$$\zeta_{J+2,J} = \zeta_{J,\epsilon} - \zeta_{J+2,\epsilon}. \quad (24)$$

Equation (21) shows that each J-component of $\langle\cos^2\theta\rangle_t$ oscillates periodically with a period $T_1 = 1/[Bc(2J+2)]$ for transitions $\Delta J=\pm1$ and $T_2 = 1/[2Bc(2J+3)]$ for transitions $\Delta J=\pm2$, and thus that $\langle\cos^2\theta\rangle_t$ periodically oscillates with the (common) period $T = 1/Bc = 20$ ps. A more detailed discussion of the re-phasing periods for alignment and orientation will be presented in the next section.

In time, $\langle\cos^2\theta\rangle_t$ oscillates around the quantity $\sum_{J,\epsilon}|C_{J,\epsilon}|^2\alpha_{J,\epsilon}$ which corresponds to a permanent or mean alignment induced by the laser pulse. This quantity is expected to approach 1/2 when the laser-induced alignment is efficient. Through the general expression (21), one can define the alignment (planar delocalization) that occurs when the two summations containing the cosine-terms are larger (smaller) than 0, such that $\langle\cos^2\theta\rangle_t$ is larger (smaller) than $\sum_{J,\epsilon}|C_{J,\epsilon}|^2\alpha_{J,\epsilon}$. The same behavior is obtained from expression (22) concerning the time evolution of the orientation. It is noted that when using hexapole state-selection and dc field orientation, the state vector contains only the low rotational J states. When populating higher rotational states with the laser field, higher frequencies are added which allow *a priori* to increase the initial degree of orientation induced by the dc field.

3. Results and discussion

Before discussing the degree of orientation that can be achieved using laser excitation, we first compare brute force orientation and orientation of state-selected NO molecules by dc electric fields. Figures 1(a) and (b) show the energy splitting and the degree of orientation for each of the two parity components of the $J=1/2$ Λ-doublet state as a function of the dc field strength. The calculation has been performed by diagonalizing the Hamiltonian in equation (17)

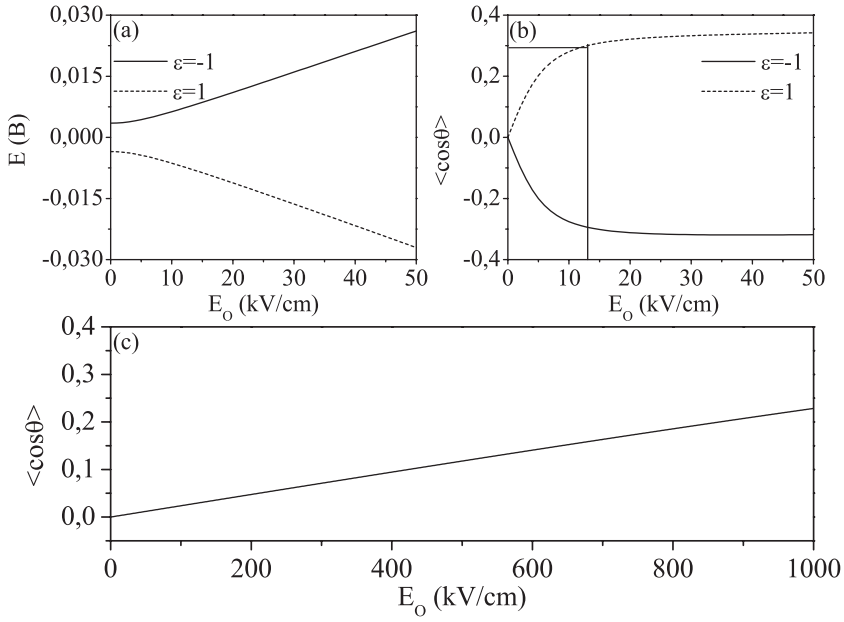

Figure 1. Stark energy (a) expressed as a fraction of the rotational NO constant $B = 1.6961\,\mathrm{cm}^{-1}$ and the degree of orientation $\langle\cos\theta\rangle$ (b) of the two parity components $\epsilon = \pm 1$ of the $J = 1/2$ ground state Λ-doublet. Note that the NO-sample remains essentially unaligned since $E_\mathrm{O} \ll B$. (c) Brute force orientation of a sample of NO molecules in their ground rotational state $J = 1/2$ that is evenly distributed over the Λ-doublet states $\epsilon = 1$ and -1. Note the impractically large value of E_O required to orient NO in (c).

without laser field. Both molecules in the low-field seeking ($\epsilon = -1$) state and molecules in the high-field seeking state ($\epsilon = 1$) that are placed in a dc field are readily oriented at moderate dc field strengths, however, their orientation is in the opposite direction. At $13\,\mathrm{kV\,cm}^{-1}$, that correspond to a dimensionless field for NO of $\omega_{E_\mathrm{O}} = 0.02$, the degree of orientation reach 0.30 for each state whereas, without state selection, no orientation is observed. A very large dc field strength is necessary to orient both types of molecules in the same direction (when directly using brute force orientation, see figure 1(c)). Also, the dipole moment of NO is rather low. For OCS molecules, $\omega_{E_\mathrm{O}} = 0.02$ is reached using only $350\,\mathrm{V\,cm}^{-1}$, meaning that for molecules with relatively high dipole moment, high degree of orientation can be reach even using a low dc field strength when hexapole state selection is applied.

The calculated time-dependent degree of alignment and orientation of NO ($J = 1/2$, $\bar{\Omega} = 1/2, \epsilon = -1$) in a $13\,\mathrm{kV\,cm}^{-1}$ electrostatic field after a 100 fs FTL laser pulse excitation is plotted in figure 2. Appreciable impulsive orientation and alignment are obtained from intensities of $3 \times 10^{12}\,\mathrm{W\,cm}^{-2}$ (top left) onwards. For intensities below $3 \times 10^{12}\,\mathrm{W\,cm}^{-2}$, the laser field is not intense enough to appreciably Raman populate the J-states that are reachable via a $\Delta J = 2$ transition. For intensities in excess of $1 \times 10^{13}\,\mathrm{W\,cm}^{-2}$ (top right), the impulsive laser excitation leads to a periodic reversal of the initial orientation prepared by the dc field, whereas for intensities in excess of $3 \times 10^{13}\,\mathrm{W\,cm}^{-2}$ (bottom left) the laser-induced orientation significantly exceeds the initial orientation by the dc electric field. The frequency of the oscillations in the orientation increases with intensity. This is particularly clear in the calculation at $1 \times 10^{14}\,\mathrm{W\,cm}^{-2}$ (bottom right), which displays high-frequency oscillations in the orientation

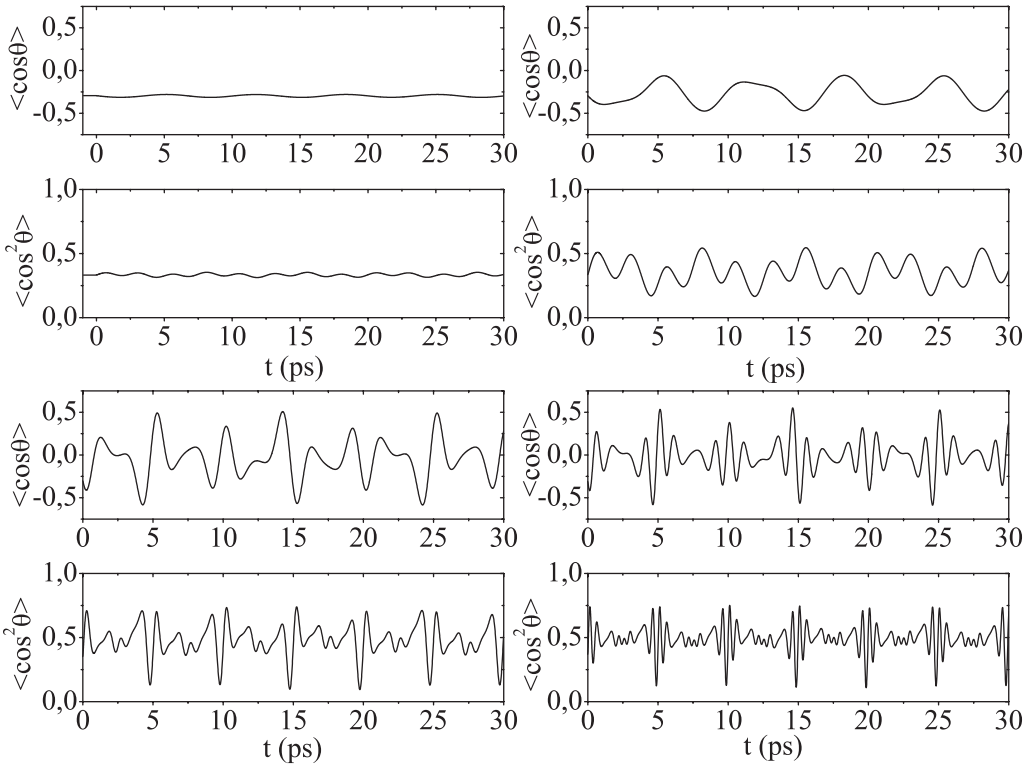

Figure 2. Degree of alignment and orientation after excitation with a FTL 100 fs, 800 nm laser pulse with intensity 3×10^{12} W cm^{-2} (top left panel pair), 1×10^{13} W cm^{-2} (top right panel pair), 4×10^{13} W cm^{-2} (bottom left panel pair) and 1×10^{14} W cm^{-2} (bottom right panel pair).

and the emergence of a revival structure, where the degree of orientation reaches a maximum every 5 ps. The laser-induced orientation of the NO molecule is accompanied by a laser-induced alignment. The revival structures occur at the same frequency in the alignment and in the orientation at 1×10^{14} W cm^{-2} (bottom right).

The occurrence of revivals in the alignment and orientation can be understood quantum mechanically in terms of the evolution of the rotational wave packet that is populated by the laser. Focusing first on the results at 1×10^{14} W cm^{-2}, we note that after the laser pulse the molecular wave function evolves via equation (19). In accordance with equations (21) and (22) orientation arises as a result of the presence of consecutive rotational levels J, ϵ and $J+1, \epsilon$ in the rotational wave packet, whereas alignment occurs when rotational level J, ϵ occurs in combination with $J+1, -\epsilon$ or $J+2, \epsilon$. Consequently it is the characteristic rephasing time T_1 between adjacent rotational levels J and $J+1$ that determines the separation between the orientation revivals, whereas the rephasing time T_2 of rotational levels J and $J+2$ determines the separation between the alignment revivals.

In the case of NO (half integer rotational states), for $J = 1/2, 3/2, 5/2, \ldots$, we find periods of $T_1 = 1/3Bc, 1/5Bc, 1/7Bc, \ldots$. These periods are all fractions of $1/Bc = 20$ ps, defining this as the first time that the wave function returns to its initial form. Hence $1/Bc$ is the rephasing time for the orientation, and the orientation maxima observed at 10 ps and 20 ps correspond to the half and full revival, respectively. Although both $\Delta J = 1$ and 2 transitions can contribute to the alignment according to equation (21), it has been shown by Meijer *et al* [53] that at

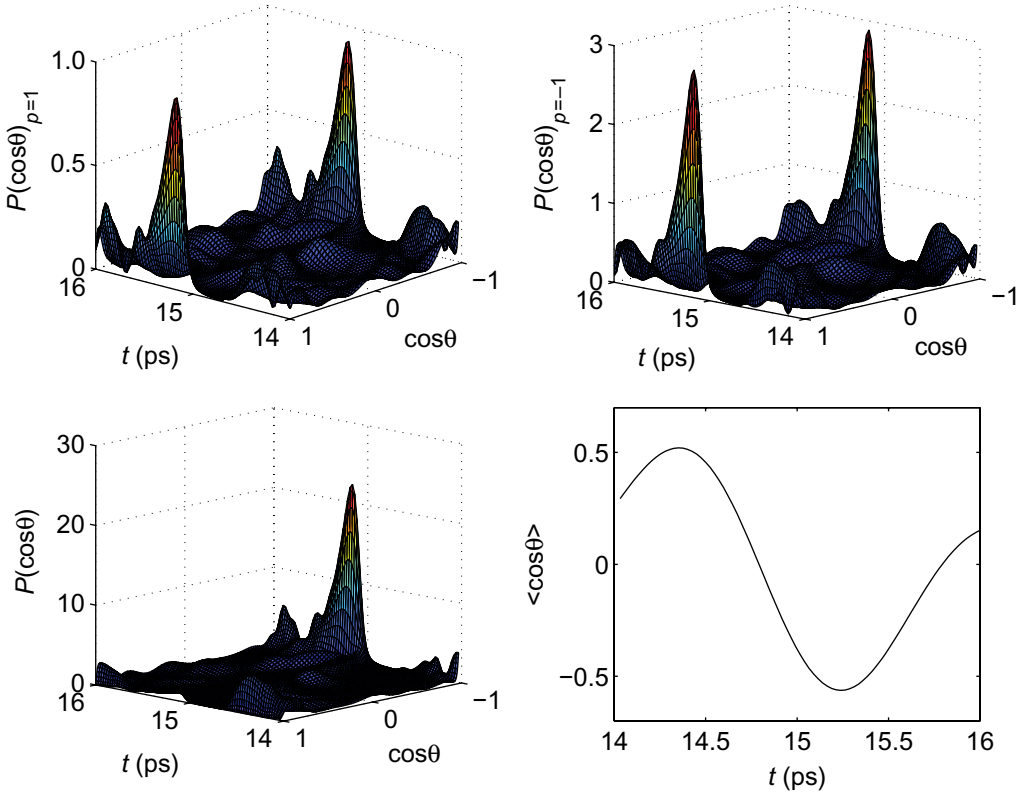

Figure 3. Probability distribution $P(\cos\theta)$ obtained for a FTL pulse of $4 \times 10^{13}\,\mathrm{W\,cm^{-2}}$ and a dc field strength of $13\,\mathrm{kV\,cm^{-1}}$. Upper panel: probability distribution for the two parity wave packet $p = \pm 1$. The distribution is symmetric with respect to $\cos\theta$ meaning that no orientation occurs. Bottom panel: total probability distribution with both parity component and corresponding $\langle\cos\theta\rangle$. When both parity components are present, the interference leads to a revival of the orientation and an asymmetric probability distribution.

high intensity the only significant $\Delta J = 1$ contribution is from $J = 1/2 \rightarrow J = 3/2$. Neglecting the $\Delta J = 1$ frequencies and focusing on $\Delta J = 2$ only, one finds for $J = 1/2, 3/2, 5/2, \ldots$ rephasing periods of $T_2 = 1/8Bc, 1/12Bc, 1/16Bc, \ldots$. Every $T = 1/4Bc$ ($= 5\,\mathrm{ps}$) the phase of all $\Delta J = 2$ contributions is a multiple of 2π, defining this as the revival time for the alignment.

As the laser field conserves the parity, it is not straightforward to understand how revivals of the orientation appear after the extinction of the laser electric field. The periodic inversion of the orientation arises from the interference between two wave packets of opposite parity that are created by the laser field. The dc field initially mixes the two parity components of the first $J = 1/2$ Λ-doublet state. As Raman transitions induced by the laser pulse conserve the parity, two wave packets of opposite parity are formed via the interaction with the short laser pulse. After the end of the pulse, these two wave packets evolve freely in time. Due to the initial coherence of the two parity components introduced by the interaction with the dc field, those two wave packets interfere which leads to revivals of the orientation at specific times, as shown in figure 3 where we have displayed both the angular distribution of the two parity wave packets

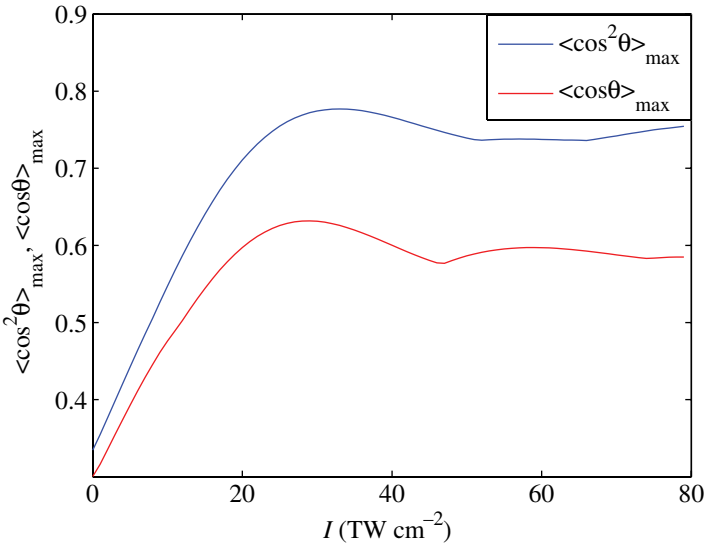

Figure 4. Evolution of the maximum value of $\langle \cos^2 \theta \rangle$ and $\langle \cos \theta \rangle$ with the laser intensity. The pulse duration is constant and equal to 100 fs.

and the final wave function at the time corresponding to the maximum of orientation. Figure 3 clearly shows that the two-parity wave packets individually are only aligned but not oriented. The coherent superposition of the two wave packets then leads to orientation of the molecule.

Figure 4 shows the dependence of the maximum impulsive orientation and alignment that can be achieved with an FTL pulse as a function of the peak laser intensity. Initially $\langle \cos^2 \theta \rangle$ and $\langle \cos \theta \rangle$ increase linearly with the peak intensity. A maximum value of the alignment (orientation) appears around 3×10^{13} W cm^{-2} and is equal to 0.775 (0.63). At higher intensities, the alignment and orientation saturate. It is also noted that at these and larger laser intensities the ionization probability of the irradiated NO molecules tends to become appreciable ($>10\%$) [54].

Several strategies have been applied in the past to enhance the degree of field-free alignment. The most common procedure consists of tailoring the laser pulse. We have used this strategy to optimize the degree of impulsive orientation. The optimization procedure is performed using an adaptive loop controlled by an evolutionary algorithm. There exist a significant number of evolutionary algorithms which differ according to, on the one hand, the strategy used to select individuals and, on the other hand, the operators which are applied to these individuals in order to create a new population. In this study, we have applied an evolutionary algorithm that was previously tested in the optimization of the alignment of simple $^1\Sigma$ diatomic molecules [55]. The DR2 Algorithm is considered to be the second generation of the so-called derandomized evolution strategies (see, e.g. [56]). It only uses mutation of parameters in order to optimize the final result. DR2 uses a linear number in the search space dimensionality n of strategy parameters as a strategy vector $\vec{\delta}^g_{\text{scal}}$, and accumulates information about the correlation or anti-correlation of past mutation vectors in order to adapt the step-size δ.

$$\vec{x}^{g+1} = \vec{x}^g + \delta^g \cdot \vec{\delta}^g_{\text{scal}} \cdot \vec{Z}, \tag{25}$$

where $\vec{Z}$ is the mutation vector, i.e. an array of random variables that are drawn from a normal distribution. In each generation the best solution generated by the mutation operator is retained,

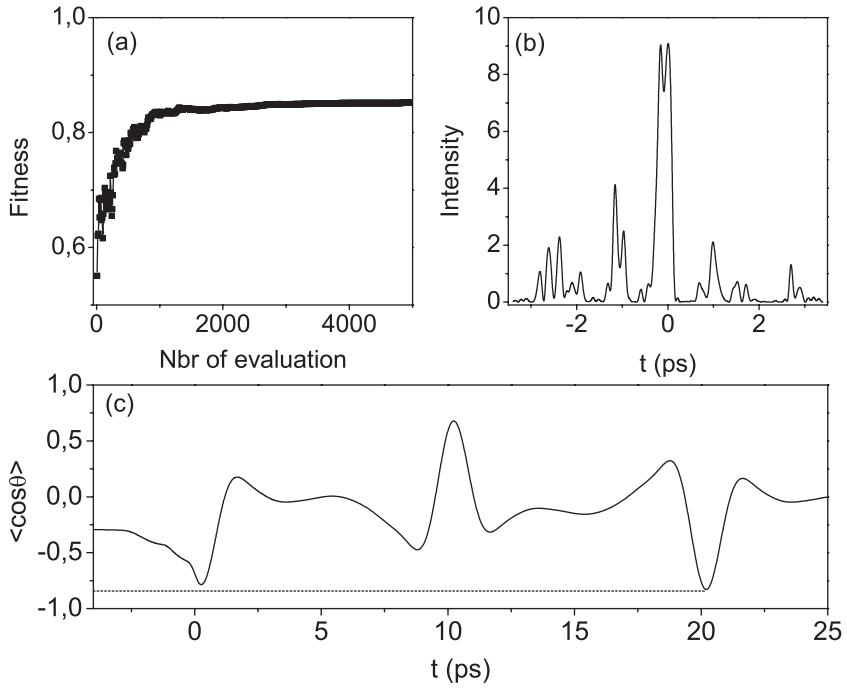

Figure 5. Optimization of the degree of orientation considering a pulse energy equivalent to a FTL pulse of $6 \times 10^{13}\,\mathrm{W\,cm^2}$ and a dc field strength of $13\,\mathrm{kV\,cm^{-1}}$. (a) Evolution of the fitness function $|\langle\cos\theta\rangle|$ versus the number of evaluations. (b) Best pulse shape that leads to the optimization of the orientation (c) and corresponding expectation value $\langle\cos\theta\rangle$.

and becomes the seed for the next generation $\vec{x}^g$. For each laser intensity 10 independent runs were performed using the DR2 algorithm. The algorithm was initialized by means of a random initialization of the phase function $\phi(\omega)$ as specified by the 128 parameters ϕ_n. Ten mutations were applied to this individual and the corresponding electric fields were evaluated. Each electric field was then tested by computing the corresponding field-free orientation evaluated using the procedure explained in section 2. Among the newly created individuals, the individual with the best degree of alignment/orientation was selected as the seed for the next generation. This procedure was repeated until convergence of the alignment/orientation was observed. Finally, only the best phase among the 10 runs performed was kept.

To mimic the experiment, the investigation was performed at constant pulse energy and at a delay corresponding to the full rotational period of NO, i.e. 20 ps. Figure 5 displays the best results of the optimization procedure starting with a FTL pulse with a peak intensity $I = 6 \times 10^{13}\,\mathrm{W\,cm^{-2}}$. As shown in this figure, the algorithm needed 1000 evaluations to reach convergence towards a value $\langle\cos\theta\rangle = 0.85$, a substantial improvement over the maximum achievable orientation with a FTL pulse ($\langle\cos\theta\rangle = 0.63$, see figure 4). Note that for this value of the orientation, six molecules are pointing in one direction for every molecule that points in the other direction. Figures 5(b) and (c) show the optimized pulse and the corresponding laser field-free molecular alignment and orientation. The particular pulse shape found by the algorithm exhibits a rather complicated structure before a main pulse center around 0 ps. The first two pulses serve to pre-orient the molecules to a value 0.6 before the main kick further increases the

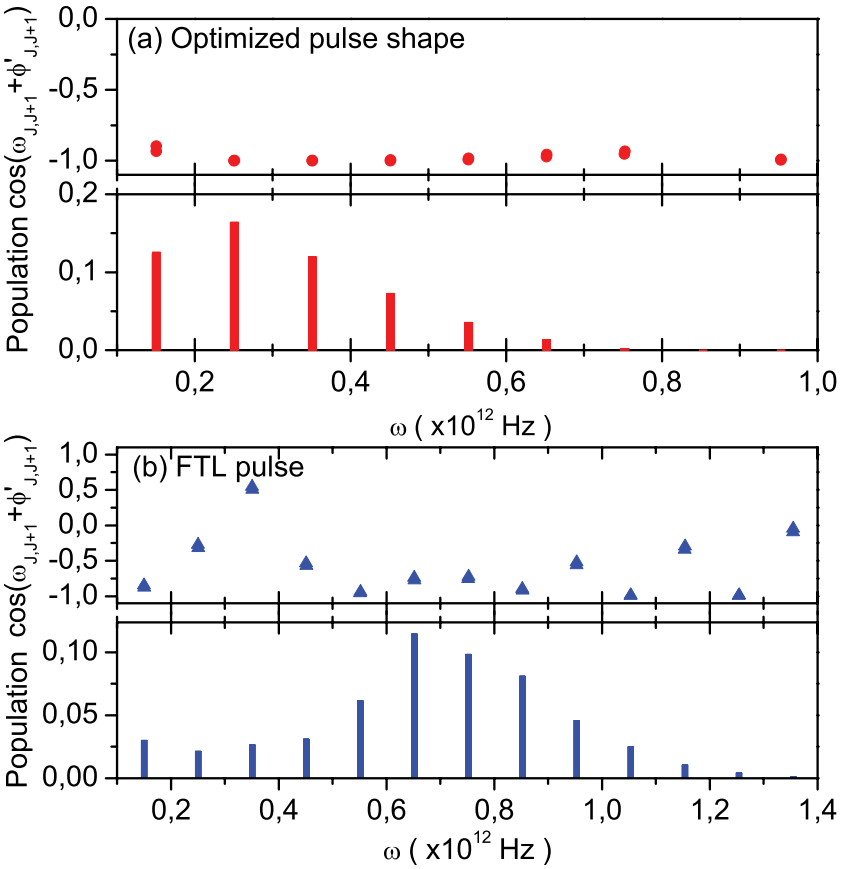

Figure 6. Rephasing terms $\cos(\omega_{J,J+1} + \zeta'_{J,J+1})$ and amplitude of the Fourier components of $\langle \cos\theta \rangle$ around $t = 20$ ps for the optimized pulse (a) and a FTL pulse of same energy (b). All the J-components of the rotational wave packet are not in phase in case of a the FTL pulse. This means that the alignment and orientation are not optimal. On the contrary, all states of the wave packet are in phase after a rotational period for the optimal pulse.

orientation. A close look at the optimized pulse shape shows that the two first pulses are centered around -1.2 and -2.6 ps. These observed time delays timing correspond to the frequency beating between states $J = 1/2$ and $5/2$ and between states $J = 5/2$ and $9/2$, respectively. It has been shown in [53] that this particular delay allows to optimize the population transfer from the initially populated $J = 1/2$ ground state to the $J = 5/2(9/2)$ state. The optimization of the molecular orientation is therefore obtained when the population distribution to the two first states accessible from a $\Delta J = 2$ transitions is efficient.

Further insight into the optimization can be obtained by looking at the population redistribution after the pulse, as well as at the rephasing term $\cos(\omega_{J,J+1} + \zeta'_{J,J+1})$ that leads to the revival of orientation (see expression (22)). Figure 6 shows that compared to a FTL pulse of same energy, the optimized laser pulse populates a lower number of states. However, in doing so, the optimized laser pulse ensures that all the components of the induced wave packet are in phase at the full revival period, in contrast with the FTL pulse, where a substantial phase-mismatch occurs between the low and the high part of the rotational distribution. The optimization algorithm therefore designs a particular pulse shape that leads to a limited

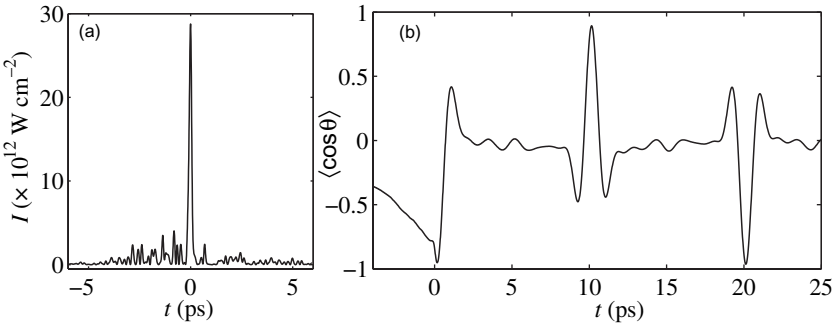

Figure 7. Optimization of the degree of orientation considering a pulse energy equivalent to a FTL pulse of $1 \times 10^{14}\,\mathrm{W\,cm^{-2}}$ and a dc field strength of $50\,\mathrm{kV\,cm^{-1}}$. (a) Best pulse shape that leads to the optimization of the orientation. It is composed of a long leading edge that pre-orient the molecule before the main pulse. (b) Corresponding expectation value $\langle\cos\theta\rangle$.

number of states involved in the rotational dynamics that are almost exactly in phase after a delay of one rotational period.

The evolutionary algorithm was applied for different laser pulse energies and dc electric field strengths. A higher degree of orientation can be achieved by increasing both the intensity and the dc field strength. The computational results revealed that meaningful optimizations are only possible if the pulse energy exceeds the pulse energy where saturation of the orientation with a FTL pulse occurs. This result is similar to what has been previously observed in case of the optimization of the molecular alignment [24]. Increasing the dc field strength leads to an increase of the static orientation and the algorithm succeeds therefore to find a better value of laser field-free orientation as well. A maximum degree of orientation of 0.964 was found using a pulse energy corresponding to a FTL pulse with a peak intensity of $I = 1 \times 10^{14}\,\mathrm{W\,cm^{-2}}$ and a dc field strength of $50\,\mathrm{kV\,cm^{-1}}$ (see figure 7). The maximum intensity of the corresponding pulse shape remains quite low ($3 \times 10^{13}\,\mathrm{W\,cm^{-2}}$), suggesting that this pulse shape could be experimentally used without significant ionization of the molecule. The laser pulse shape in figure 7 is even more complicated than the one shown previously, in figure 6, at the lower intensity. In particular, in the build-up of the laser field prior to the main pulse well-defined sub-pulses that appear at times that can be related to the rotational structure can no longer be identified. Rather, ahead of the main pulse, the laser field displays a gradual build-up that leads to an adiabatic pre-orientation of the molecule. The calculation thereby reproduces an observation that was previously obtained for the case of molecular alignment, namely that 'ultimate' orientation requires the sequence of an adiabatic and a non-adiabatic laser interaction [57]. We note that the laser pulse shape shown in figure 7 has characteristics that are out of reach when using sigmoidal phase-shaping, as was experimentally done in [49]. Sigmoidal phase-shaping leads to a pulse shape that is qualitatively similar to the pulse shapes shown in figures 6 and 7, namely, a slow rise followed by a short and intense main pulse. However, using sigmoidal phase shaping the slow rise starts at -2 ps before the main pulse, whereas in figure 7 the optimized pulse starts at -5 ps. Therefore, a sigmoidal phase can provide a suitable initial guess of the phase that is to be applied to obtain optimal orientation, but further optimization under the guidance of an evolutionary algorithm is necessary to reach optimal results.

4. Conclusion

In conclusion, we have shown that using a hexapole state selector to produce a sample of state-selected molecules, combined with the application of a dc field and a short laser pulse, a very high degree of orientation can be achieved even for a molecule with a small dipole moment like NO. By applying an adaptive loop that mimics the feedback loop in a pulse shaping experiment, we have shown that an unprecedented degree of orientation can be reached. With the availability of a high degree of field-free orientation, molecular frame photoelectron imaging experiments and molecular frame studies of reaction dynamics of heteronuclear molecules become possible.

Acknowledgments

This work is part of the research program of the 'Stichting voor Fundamenteel Onderzoek der Materie (FOM)', which is financially supported by the 'Nederlandse organisatie voor Wetenschappelijk Onderzoek (NWO)'.

Appendix A. Coupling coefficients

The coupling coefficient of $\cos\theta$ and $\cos^2\theta$ in the NO rotational basis $|J\bar{\Omega}M\epsilon\rangle$ are obtained using the following procedure. Using

$$\cos\theta = P_1(\cos\theta) \quad \text{and} \quad \cos^2\theta = \tfrac{2}{3}P_2(\cos\theta) + \tfrac{1}{3},$$

we can rewrite the total Hamiltonian from equation (17) as

$$\begin{aligned} H^{M,\bar{\Omega}}_{J,J',\epsilon,\epsilon'} &= \langle J', \bar{\Omega}, M, \epsilon'|H_{\text{rot}} - \omega P_1(\cos\theta) - \tfrac{2}{3}\Delta\omega P_2(\cos\theta)|J, \bar{\Omega}, M, \epsilon\rangle \\ &= \delta_{J,J'}\delta_{\epsilon,\epsilon'}E_{\text{rot}} - \omega Q_1(J', J, M, \bar{\Omega}, \epsilon', \epsilon) + \tfrac{2}{3}\Delta\omega Q_2(J', J, M, \bar{\Omega}, \epsilon', \epsilon), \end{aligned} \tag{A.1}$$

with for $n = 1, 2$:

$$\begin{aligned} Q_n(J', J, M, \bar{\Omega}, \epsilon', \epsilon) &= \langle J'\bar{\Omega}M\epsilon'|P_n(\cos\theta)|J\bar{\Omega}M\epsilon\rangle \\ &= \tfrac{1}{2}[\langle J'\bar{\Omega}M|D^n_{00}|J\bar{\Omega}M\rangle + \epsilon\epsilon'\langle J' - \bar{\Omega}M|D^n_{00}|J - \bar{\Omega}M\rangle]. \end{aligned} \tag{A.2}$$

$D^n_{00} = P_n(\cos\theta)$ is a Wigner rotation matrix element. Substitution of equation (3) and subsequent application of equation (3.118) of [50] leads to:

$$\begin{aligned} Q_n(J', J, M, \bar{\Omega}, \epsilon', \epsilon) = \frac{1}{2}\sqrt{(2J+1)(2J'+1)} \times \begin{pmatrix} J' & n & J \\ M & 0 & -M \end{pmatrix} \\ \left[(-1)^{M-\bar{\Omega}}\begin{pmatrix} J' & n & J \\ \bar{\Omega} & 0 & -\bar{\Omega} \end{pmatrix} + (-1)^{M+\bar{\Omega}}\,\epsilon\epsilon'\begin{pmatrix} J' & n & J \\ -\bar{\Omega} & 0 & \bar{\Omega} \end{pmatrix}\right]. \end{aligned} \tag{A.3}$$

With this expression and equation (20), we can immediately write the degree of orientation ($n = 1$) and alignment ($n = 2$) at every moment after the laser pulse:

$$\begin{aligned} \langle P_n(\cos\theta)\rangle &= \langle\Psi(t)|P_n(\cos\theta)|\Psi(t)\rangle \\ &= \sum_{J'\epsilon'} C^{M\bar{\Omega}*}_{J',\epsilon'}\, C^{M\bar{\Omega}}_{J,\epsilon} e^{-i(E_{\text{rot}}(J') - E_{\text{rot}}(J))\,(t-t_f)/\hbar}\, Q_n(J', J, M, \bar{\Omega}, \epsilon', \epsilon). \end{aligned} \tag{A.4}$$

In this last expression, $J' = J$ will lead to the coupling coefficient with $\Delta J = 0$ whereas $J' = J+1$ and $J' = J+2$ will lead to the coupling coefficient that verify $\Delta J = 1$ and $\Delta J = 2$, respectively. Using table 2.5 of [50] that gives an analytic expression of the $3-j$ symbols, expression (A.3) can be developed and we finally find

$$\alpha_{J,\epsilon}^{M,\bar{\Omega}} = \langle J, \bar{\Omega}, M, \epsilon | \cos^2\theta | J, \bar{\Omega}, M, \epsilon \rangle = \left[\frac{M\bar{\Omega}}{J(J+1)}\right]^2 + \frac{1}{(J+1)^2}\frac{((J+1)^2 - M^2)((J+1)^2 - \bar{\Omega}^2)}{(2J+1)(2J+3)} + \frac{1}{J^2}\frac{(J^2 - M^2)(J^2 - \bar{\Omega}^2)}{(2J+1)(2J-1)}, \tag{A.5}$$

$$\gamma_{J+1,\epsilon}^{M,\bar{\Omega}} = \langle J+1, \bar{\Omega}, M, -\epsilon | \cos^2\theta | J, \bar{\Omega}, M, \epsilon \rangle = \frac{M\bar{\Omega}}{2J(J+1)(J+2)}\left[\frac{((J+1)^2 - M^2)((J+1)^2 - \bar{\Omega}^2)}{(2J+1)(2J+3)}\right]^{1/2}, \tag{A.6}$$

$$\beta_{J+2,\epsilon}^{M,\bar{\Omega}} = \langle J+2, \bar{\Omega}, M, \epsilon | \cos^2\theta | J, \bar{\Omega}, M, \epsilon \rangle = \frac{1}{(J+1)(J+2)}\left[\frac{((J+1)^2 - M^2)((J+1)^2 - \bar{\Omega}^2)}{(2J+3)^2}\right]^{1/2} \times \left[\frac{((J+2)^2 - M^2)((J+2)^2 - \bar{\Omega}^2)}{(2J+1)(2J+5)}\right]^{1/2}. \tag{A.7}$$

References

[1] Kramer K H and Bernstein R B 1965 Focusing and orientation of symmetric-top molecules with the electric six-pole field *J. Chem. Phys.* **42** 767–70

[2] Brooks P R 1976 Reactions of oriented molecules *Science* **193** 11

[3] Kuipers E W, Tenner M G, Kleyn A W and Stolte S 1988 Observation of steric effects in gas-surface scattering *Nature* **334** 420–2

[4] Friedrich B and Herschbach D 1995 Polarization of molecules induced by intense nonresonant laser fields *J. Phys. Chem.* **99** 15686–93

[5] Ortigoso J, Rodriguez M, Gupta M and Friedrich B 1999 Time evolution of pendular states created by the interaction of molecular polarizability with a pulsed nonresonant laser field *J. Chem. Phys.* **110** 3870

[6] Rosca-Pruna F and Vrakking M J J 2001 Experimental observation of revival structures in picosecond laser-induced alignment of I_2 *Phys. Rev. Lett.* **87** 153902

[7] Hamilton E, Seideman T, Ejdrup T, Poulsen M D, Bisgaard C Z, Viftrup S S and Stapelfeldt H 2005 Alignment of symmetric top molecules by short laser pulses *Phys. Rev.* A **72** 043402

[8] Vrakking M J J and Stolte S 1997 Coherent control of molecular orientation *Chem. Phys. Lett.* **217** 209–15

[9] Baumfalk R, Nahler N H and Buck U 2001 Photodissociation of oriented HXeI molecules in the gas phase *J. Chem. Phys.* **114** 4755–8

[10] Sakai H, Minemoto S, Nanjo H, Tanji H and Suzuki T 2003 Controlling the orientation of polar molecules with combined electrostatic and pulsed, nonresonant laser fields *Phys. Rev. Lett.* **90** 83001

[11] Friedrich B, Nahler N H and Buck U 2003 The pseudo-first-order stark effect and the orientation of HXeI molecules *J. Mod. Optics* **50** 2677–89

[12] Rakitzis T P, van den Brom A J and Janssen M H M 2004 Directional dynamics in the photodissociation of oriented molecules *Science* **303** 1852–4
[13] Taatjes C A, Gijsbertsen A, de Lange M J L and Stolte S 2007 Measurements and quasi-quantum modeling of the steric asymmetry and parity propensities in state-to-state rotationally inelastic scattering of NO ($^2\Pi_{1/2}$) with D_2 *J. Phys. Chem.* A **111** 7631–9
[14] Loesch H J and Remscheid A 1990 Brute force in molecular reaction dynamics: a novel technique for measuring steric effects *J. Chem. Phys.* **93** 4779–90
[15] Friedrich B and Herschbach D 1991 On the possibility of orienting rotationally cooled polar molecules in an electric field *Z. Phys.* D **18** 153–61
[16] Bulthuis J, van leuken J J and Stolte S 1995 Hexapole state selection and focusing vs brute force orientation of beam molecules *J. Chem. Soc. Faraday Trans.* **91** 205–14
[17] Normand D, Lompre L A and Cornaggia C 1992 Laser-induced molecular alignment probed by a double-pulse experiment *J. Phys. B: At. Mol. Opt. Phys.* **25** L497–503
[18] Stapelfeldt H and Seideman T 2003 Colloquium: aligning molecules with strong laser pulses *Rev. Mod. Phys.* **75** 543
[19] Sakai H, Safvan C P, Larsen J J, Hilligsoe K M, Hald K and Stapelfeldt H 1999 Controlling the alignment of neutral molecules by a strong laser field *J. Chem. Phys.* **110** 10235–8
[20] Larsen J J, Sakai H, Safvan C P, Wendt-Larsen I and Stapelfeldt H 1999 Aligning molecules with intense nonresonant laser fields *J. Chem. Phys.* **111** 7774
[21] Seideman T 1999 Revival structure of aligned rotational wave packets *Phys. Rev. Lett.* **83** 4971–4
[22] Leibscher M, Averbukh I Sh and Rabitz H 2003 Molecular alignment by trains of short laser pulses *Phys. Rev. Lett.* **90** 213001
[23] Bisgaard C Z, Poulsen M D, Péronne E, Viftrup S S and Stapelfeldt H 2004 Observation of enhanced field-free molecular alignment by two laser pulses *Phys. Rev. Lett.* **92** 173004
[24] Hertz E, Rouzée A, Guérin S, Lavorel B and Faucher O 2007 Optimization of field-free molecular alignment by phase-shaped laser pulses *Phys. Rev.* A **75** 031403
[25] Suzuki T, Sugawara Y, Minemoto S and Sakai H 2008 Optimal control of nonadiabatic alignment of rotationally cold N_2 molecules with the feedback of degree of alignment *Phys. Rev. Lett.* **100** 033603
[26] Velotta R, Hay N, Mason M B, Castillejo M and Marangos J P 2001 High-order harmonic generation in aligned molecules *Phys. Rev. Lett.* **87** 183901
[27] Meckel M *et al* 2008 Laser-induced electron tunneling and diffraction *Science* **320** 1478–82
[28] Itatani J, Levesque J, Zeidler D, Niikura H, Pépin H, Kieffer J C, Corkum P B and Villeneuve D M 2004 Tomographic imaging of molecular orbitals *Nature* **432** 867–71
[29] Torres R *et al* 2007 Probing orbital structure of polyatomic molecules by high-order harmonic generation *Phys. Rev. Lett.* **98** 203007
[30] Kanai T, Minemoto S and Sakai H 2005 Quantum interference during high-order harmonic generation from aligned molecules *Nature* **435** 470–4
[31] Larsen J J, Hald K, Bjerre N, Stapelfeldt H and Seideman T 2000 Three dimensional alignment of molecules using elliptically polarized laser fields *Phys. Rev. Lett.* **85** 2470
[32] Viftrup S S, Kumarappan V, Trippel S, Stapelfeldt H, Hamilton E and Seideman T 2007 Holding and spinning molecules in space *Phys. Rev. Lett.* **99** 143602
[33] Lee K F, Villeneuve D M, Corkum P B, Stolow A and Underwood J G 2006 Field-free three-dimensional alignment of polyatomic molecules *Phys. Rev. Lett.* **97** 173001
[34] Underwood J G, Sussman B J and Stolow A 2005 Field-free three dimensional molecular axis alignment *Phys. Rev. Lett.* **94** 143002
[35] Rouzée A, Guérin S, Faucher O and Lavorel B 2008 Field-free molecular alignment of asymmetric top molecules using elliptically polarized laser pulses *Phys. Rev.* A **77** 043412
[36] Dion C M, Bandrauk A D, Atabek O, Keller A, Umeda H and Fujimura Y 1999 Two-frequency ir laser orientation of polar molecules, numerical simulations for hcn *Chem. Phys. Lett.* **302** 215–23

[37] Kanai T and Sakai H 2001 Numerical simulations of molecular orientation using strong nonresonant, two-colour laser fields *J. Chem. Phys.* **115** 5492–97
[38] Machholm M and Henriksen N E 2001 Field-free orientation of molecules *Phys. Rev. Lett.* **87** 193001
[39] Dion C M, Keller A and Atabek O 2001 Orienting molecules using half-cycle pulses *Eur. Phys. J.* D **14** 239–255
[40] Daems D, Guérin S, Sugny D and Jauslin H R 2005 Efficient and long-lived field-free orientation of molecules by a single hybrid short pulse *Phys. Rev. Lett.* **94** 153003
[41] Gershnabel E, Averbukh I Sh and Gordon R J 2006 Enhanced molecular orientation induced by molecular antialignment *Phys. Rev.* A **74** 053414
[42] Leemans W P, Nagler B, Gonsalves A J, Tòth Cs, Nakamura K, Geddes C G R, Esarey E, Schroeder C B and Hooker S M 2006 Gev electron beams from a centimetre-scale accelerator *Nat. Phys.* **2** 696–9
[43] Friedrich B and Herschbach D 1999 Enhanced orientation of polar molecules by combined electrostatic and nonresonant induced dipole forces *J. Chem. Phys.* **111** 6157
[44] Friedrich B and Herschbach D 1999 Manipulating molecules via combined static and laser fields *J. Phys. Chem.* A **103** 10280–8
[45] Cai L, Marango J and Friedrich B 2001 Time-dependent alignment and orientation of molecules in combined electrostatic and pulsed nonresonant laser fields *Phys. Rev. Lett.* **86** 775–8
[46] Tanji H, Minemoto S and Sakai H 2005 Three-dimensional molecular orientation with combined electrostatic and elliptically polarized laser fields *Phys. Rev.* A **72** 063401
[47] Goban A, Minemoto S and Sakai H 2008 Laser-field-free molecular orientation *Phys. Rev. Lett.* **101** 013001
[48] Holmegaard L, Nielsen J H, Nevo I, Stapelfeldt H, Filsinger F, Küpper J and Meijer G 2009 Laser-induced alignment and orientation of quantum-state-selected large molecules *Phys. Rev. Lett.* **102** 023001
[49] Ghafur O, Rouzée A, Gijsbertsen A, Siu W, Stolte S and Vrakking M J J 2009 Impulsive orientation and alignment of quantum state-selected no molecules *Nat. Phys.* **5** 1225
[50] Zare R N 1988 *Angular Momentum: Understanding Spatial Aspects in Chemisty and Physics* (New York: Wiley)
[51] Burrus C A and Gordy W 1953 One-to-two millimeter wave spectroscopy. III. NO and DI *Phys. Rev.* **92** 1437–9
[52] Gijsbertsen A, de Lange M J L, Wiskerke A E, Linnartz H, Drabbels M, Kłos J and Stolte S 2004 Sign of the state-to-state steric asymmetry of rotationally-inelastic atom-molecule collisions *Chem. Phys.* **301** 293
[53] Meijer A S, Zhang Y, Parker D H, van der Zande W J, Gijsbertsen A and Vrakking M J J 2007 Controlling rotational state distributions using two-pulse stimulated raman excitation *Phys. Rev.* A **76** 023411
[54] Larochelle S, Talebpour A and Chin S L 1997 Non-sequential and sequential double ionization of no in an intense femtosecond ti:sapphire laser pulse *J. Phys. B: At. Mol. Opt. Phys.* **30** L245
[55] Shir O M, Beltrani V, Bäck Th, Rabitz H and Vrakking M J J 2008 On the diversity of multiple optimal controls for quantum systems *J. Phys. B: At. Mol. Opt. Phys.* **41** 074021
[56] Hansen N and Ostermeier A 2001 *Evol. Comput.* **9** 159
[57] Guérin S, Rouzée A and Hertz E 2008 Ultimate field-free molecular alignment by combined adiabatic-impulsive field design *Phys. Rev.* A **77** 041404